Nuclear Instruments and Methods in Physics Research B 546 (2024) 165147

Contents lists available at ScienceDirect

Nuclear Inst. and Methods in Physics Research, B

journal homepage: www.elsevier.com/locate/nimb

Slit extraction and emittance results of a permanent magnet minimum-B quadrupole electron cyclotron resonance ion source

Sami Kosonen [a,*], Taneli Kalvas [a], Hannu Koivisto [a], Olli Tarvainen [b], Ville Toivanen [a]

[a] Department of Physics, Accelerator laboratory, University of Jyväskylä, Jyväskylä, FI-40014, Finland
[b] STFC-UKRI Pulsed Spallation Neutron and Muon Facility, Rutherford Appleton Laboratory, Harwell, OX110QX, UK

ARTICLE INFO

Dataset link: https://doi.org/10.23729/c5abab71-5277-48d6-a9c2-78101bf58e70

Keywords:
Ion source
Electron cyclotron resonance
Ion beam
Plasma confinement
Emittance
Beam extraction

ABSTRACT

We present an experimental and simulation study of high charge state ion beams produced with a permanent magnet electron cyclotron resonance ion source (ECRIS) with minimum-B quadrupole magnetic field topology and slit extraction system. The unconventional topology generates fan-shaped plasma flux, favouring a rectangular aperture for beam extraction. We demonstrate successful low-energy transport of the slit beam, achieving up to 25 times higher beam currents compared to a round extraction aperture. Maximum beam intensities are 1.5 and 15 μA for argon 11+ and 9+, respectively. The results indicate microwave power-limited beam production. Emittance values are comparable to traditional ECRIS. Unlike in conventional ECRIS, the emittance increases monotonically with increasing charge state due to slit extraction, magnetic topology, and beam transport characteristics. The experimental transport efficiency for helium ranges from 32% to 50%, depending on the total beam current. The losses primarily occur due to the dipole magnet's insufficient vertical aperture.

1. Introduction

The CUBE-ECRIS is a permanent magnet minimum-B quadrupole electron cyclotron resonance ion source recently designed and built at the JYFL (University of Jyväskylä, Department of Physics) accelerator laboratory [1,2]. The main difference between the CUBE-ECRIS and conventional minimum-B ECR ion sources is the magnetic field topology. Conventional ECR ion sources utilize a superposition of solenoid and sextupole fields, resulting in efficient electron heating at a closed resonance surface, magnetic confinement of the electrons, and suppression of magnetohydrodynamic instabilities. The magnet design of the CUBE-ECRIS has been inspired by the experimental "yin-yang" or "baseball seam" devices used for mirror confinement fusion plasma research [3–5], and a more recent incarnation of the "yin-yang" quadrupole minimum-B, the 6.4 GHz ARC-ECRIS [6], demonstrating the production of argon ion beams up to 6+ charge state. In these devices the quadrupole field topology is produced with "combined function" electromagnets instead of using separate solenoid and quadrupole magnets as was done for the 10 GHz Quadrumafios ion source reaching argon charge states up to 11+ [7].

The CUBE-ECRIS operating in the frequency range of 10–11.5 GHz has been built for two purposes. First, it is intended to demonstrate high charge state ion production at X-band microwave frequencies and, thus, act as an intermediate step between the first 6.4 GHz ARC-ECRIS prototype [6] and potential superconducting versions of the concept feasible up to 100 GHz [8]. Second, being an all-permanent magnet ECRIS the CUBE source is a viable candidate for a "net-zero", SF_6-free single-ended low energy time-of-flight elastic recoil detection analysis (ToF-ERDA) facility using high charge state noble gas ions [9], where the beam current requirements are not as stringent as in typical nuclear physics applications.

The first experimental results taken on the CUBE-ECRIS are presented in Ref. [2] and can be summarized into three key findings: (i) electron heating up to ~200 KeV energies, (ii) electrostatic confinement of high charge state ions, and (iii) production of high charge state ion beams up to Ar^{11+} and beam currents of at least 1 μA for Ar^{9+} and lower charge states.

In those first experiments the extraction aperture was an 8 mm diameter round hole, which does not match the escaping, fan-shaped plasma flux forming a distinct strip pattern at the plane of the plasma electrode, characteristic to the quadrupole field topology. As explained in detail in Ref. [1], the preferred shape of the plasma electrode aperture is a rectangular slit, which, however, complicates the downstream beam transport. In this paper we report experimental results, i.e. beam currents and emittance of argon ion beams extracted from the CUBE-ECRIS, using a slit-aperture extraction for the first time. The results are compared to those obtained with the round aperture and to

* Corresponding author.
E-mail address: satakoso@jyu.fi (S. Kosonen).

https://doi.org/10.1016/j.nimb.2023.165147
Received 26 June 2023; Received in revised form 20 October 2023; Accepted 23 October 2023
Available online 4 November 2023

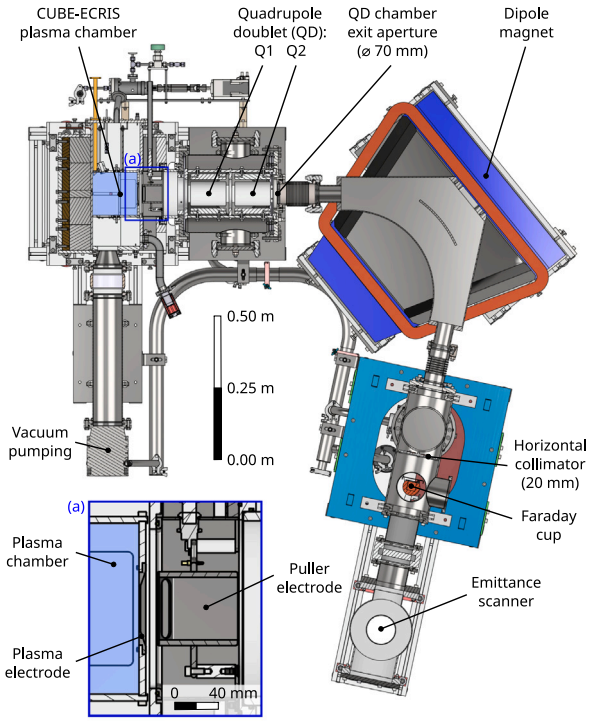

Fig. 1. A cross section view of the CUBE-ECRIS and the low energy beam transport. The collimator upstream from the Faraday cup restricts the beam size only in horizontal (x) direction. A detailed view of the beam extraction region is presented in subfigure (a) with a slit-extraction plasma electrode (40 mm × 4 mm aperture).

emittance trends (charge state dependence) observed in conventional ECR ion sources. Finally, we discuss the transport efficiency of the ion beams. The conclusions are supported by extraction and beam transport simulations.

2. Experimental setup and procedure

The CUBE-ECRIS and its low energy beam transport (LEBT) including diagnostics are presented in Fig. 1.

The details of the ion source magnetic field can be found in Ref. [1]. The microwave radiation (RF) sustaining the plasma is generated with a Keysight EXG Analog Signal Generator N5173B and amplified with a XICOM Technology XTRD-450I Travelling Wave Tube Amplifier (TWTA). The amplifier is connected to the CUBE-ECRIS plasma chamber via a WR75 rectangular wave guide transmission line equipped with a high voltage break and a vacuum window. As the magnetic field structure of CUBE-ECRIS cannot be varied, the microwave frequency is a significant plasma tuning parameter to optimize the source performance. Here the frequency was varied between 10 and 11.5 GHz. In this frequency range the TWTA provides a maximum RF power of about 300 W The gas feed rate into the plasma chamber is controlled with two independent precision valves, allowing operation with two gas species. The two biased discs are circular, d = 20 mm stainless steel inserts insulated from the plasma chamber wall. The biased discs are located at the maxima of the plasma flux loss line as per the electron tracing simulations of Ref. [1] (for further details, see the Supplementary Data of [2]).

The CUBE-ECRIS has been designed for extraction voltages around 10 kV. The plasma electrode is a separate plate embedded to the plasma chamber wall (see subplot (a) in Fig. 1) allowing the extraction aperture to be changed. Three different extraction apertures were used in this study; a round aperture with 8 mm diameter and two rectangular slit apertures with horizontal × vertical dimensions of 20 mm × 4 mm and 40 mm × 4 mm. Facing the plasma electrode is a puller electrode with a 55 mm × 8 mm slit aperture. The puller electrode can be biased negatively with respect to the ground potential, which increases the electric field strength in the acceleration gap. The horizontal slit beam rotates to roughly vertical in the extraction due to decreasing magnetic field of the ion source.

An electrostatic quadrupole doublet is located immediately downstream from the extraction system. The quadrupoles were intended for matching the extracted beam into the following dipole with ∼1 kV voltages as presented in [1]. However, the experimental optimum was found at significantly lower voltages (around 100 V for Q1 and 0 V for Q2) for high charge states of argon.

The ion beams are mass-to-charge (M/Q) analysed using a 102° spectrometer dipole magnet with a 350 mm turning radius and 70 mm pole gap. The free height of the vacuum chamber is 60 mm. The ion currents are measured with a Faraday cup downstream from the magnet. The Faraday cup is equipped with secondary electron suppression and its entrance is 98 mm in vertical and 28 mm in horizontal direction to accommodate the expected shape of the slit-extracted and rotated ion beams. A 20 mm horizontal collimator is placed in front of the Faraday cup to improve the resolution. The charge state distribution of the extracted beams is determined by sweeping the magnetic field of the spectrometer magnet and measuring the ion current from the Faraday cup. This measurement setup was used with all extraction aperture setups.

The vertical (y, y') and horizontal (x, x') emittances of M/Q-analysed beams were measured with an Allison-type emittance scanner [10] located downstream from the dipole magnet, as shown in Fig. 1. Here the vertical direction means “up-down” or “in and out of page” in Fig. 1. Switching between the horizontal and vertical measurement planes requires breaking the beamline vacuum and physically rotating the emittance scanner. As implied, with Allison type scanners only two-dimensional measurement are possible, from which the cross-correlations between the (y, y’) and (x, x’) are impossible to entangle. This is relevant for example in the case of beam rotation, which is discussed hereafter. An essential part of the emittance measurement is the data analysis, where for example the artefacts such as amplifier bias and background noise are removed [11]. Firstly, the average value of the background was calculated using the SCUBEEx method [12], and then removed from the data. Next, the data was thresholded i.e. the measurement points with values below a certain threshold percentage from the maximum intensity were reset to zero. In this study the threshold values were between 5–10%. Finally, cluster analysis [13] was used to remove possible ghost signals in the data. Determining the exact values for the thresholding percentage and cluster-removal filter, i.e. the minimum relative intensity of a separate cluster and the global intensity maximum, has to be done by experimenting with the values and visually inspecting the resulting phase space distribution plots [11]. Blindly trusting the algorithm may cause wrong interpretations. For example, if the phase space distributions measured as a function of a parameter, such as the RF power, have aberrations, the algorithm may delete these only from some distributions, which could lead to wrong conclusions about the parametric trends seen in the data.

All data described hereafter were collected with 10 kV source potential and with the source control parameters, e.g. bias disc voltage and gas pressure, optimized for the production of $^{40}Ar^{9+}$. The experiments were started with the 8 mm diameter round extraction aperture, which provides a reasonable comparison to conventional ECR ion source extraction systems. The charge state distribution (CSD) and (y, y') and (x, x') emittances of the resulting beams (charge states) were then measured. Next, the extraction aperture was changed to a 20 mm × 4 mm rectangular slit and the measurements were repeated. This acts as an intermediate step towards the “nominal” 40 mm wide slit. The bulk of the data were collected with the 40 mm × 4 mm rectangular slit aperture. This is the aperture size for which the CUBE-ECRIS beam extraction and transport systems have been designed for, based on the

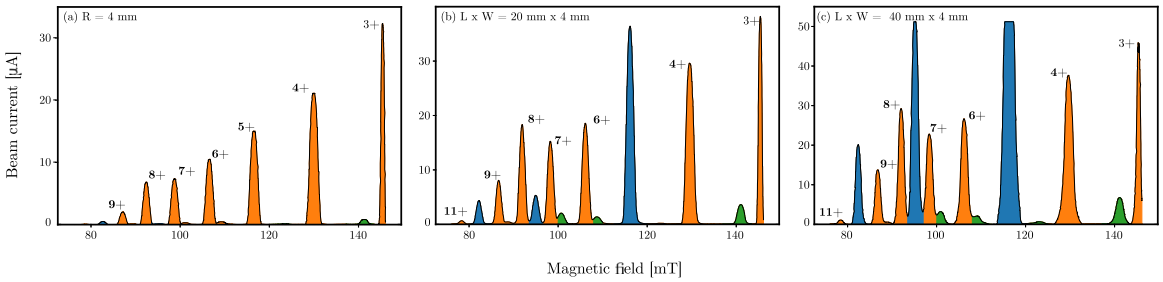

Fig. 2. Argon charge state distributions for (a) round 8 mm diameter aperture, (b) rectangular 20 mm × 4 mm slit aperture and (c) rectangular 40 mm × 4 mm slit aperture with 270–280 W microwave power. The ion source parameters were optimized for Ar^{9+} in each case. The total extracted beam currents (HV drain currents) were 0.28 mA, 0.39 mA and 1.45 mA, respectively, for (a), (b) and (c). The argon "peaks" are highlighted with orange, oxygen with blue and impurities (carbon and nitrogen) with green. Notice the different beam current scale in each CSD.

ion optical simulations [1]. With the large slit we applied oxygen as a mixing gas and biased the puller electrode to ∼−3 kV potential (neither being implemented for the other two apertures). These two changes mitigated extraction stability issues observed otherwise. The negative bias in the puller electrode also affects the space charge compensation, but we expect the effect to be small and local. The ion source was optimized for the production of $^{40}Ar^{9+}$ with 280 W RF power and the CSD of the beam extracted from the Ar+O plasma was measured in the RF power range from 50 to 280 W. The (y, y') and (x, x') emittances of different argon charge states were also measured with several RF powers.

Finally, the beam transport was studied further by measuring the transmission efficiency of helium ions extracted from the CUBE-ECRIS plasma to the Faraday cup downstream from the spectrometer magnet. This measurement was performed with helium in order to be able to transport both charge states ($^4He^+$ and $^4He^{2+}$) through the spectrometer magnet with 10 kV extraction voltage, −2.6 kV puller voltage and the 40 mm × 4 mm slit extraction aperture. The total extracted beam current (power source drain current) was varied from 0.4 to 1.6 mA by adjusting the RF power between 4 and 200 W.

3. Results

3.1. Beam current measurements

Charge state distributions (CSD) of argon with 10 kV extraction voltage and 270–280 W RF power at 10.5 GHz are shown in Fig. 2 where (a) is with the 8 mm diameter round aperture, (b) with the rectangular slit aperture of 20 mm × 4 mm and (c) with 40 mm × 4 mm slit. Gas mixing with oxygen was applied in (c) as explained above. The CSDs exhibit major improvement of all argon charge state currents when the rectangular slit apertures are compared to the round aperture. Especially the high charge state (8+, 9+ and 11+) beam currents are many times higher with the slit, up to a factor of 25 for Ar^{11+} as shown in Table 1. We note that Ar^{10+} overlaps with O^{4+} and, thus, is not shown here. Approximately twofold improvement is observed when comparing the smaller 20 mm × 4 mm rectangular slit to the bigger 40 mm × 4 mm slit. The beam current improvement depends on the charge state, i.e. the higher the CS the bigger the improvement. Possible reasons for the observed scaling are: the shape of the escaping plasma flux (the particle distribution incident on the extraction aperture), gas mixing (with the 40 mm × 4 mm slit), collimation on the puller and potentially different transport efficiencies of different argon beams. We draw the attention to the fact that the CSDs optimized for Ar9+ peak at lower charge states and are different to those in classical ECR ion sources.

It is noted that the beam currents shown in Table 1 for the 8 mm diameter case are significantly higher than what was reported in Ref. [2] for the same aperture. This is mainly due to changes made to the microwave transmission line, which resulted in better coupling and transmission efficiency, and made the previously inaccessible frequencies available to be used in this study.

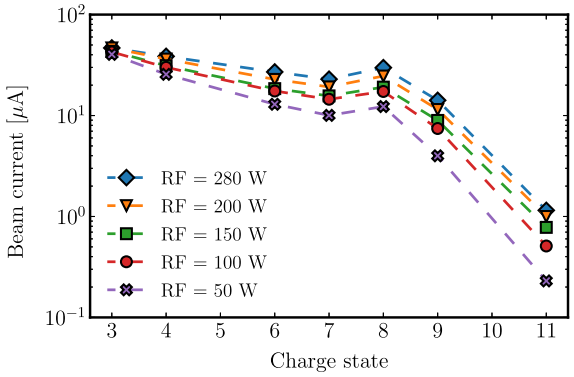

Fig. 3. Argon beam currents of different charge states at different RF powers with the 40 mm × 4 mm rectangular slit aperture. The ion source was tuned for the CS 9+ at the highest RF power.

Table 1
The highest beam currents of argon charge states 8+, 9+ and 11+ achieved with each plasma electrode aperture.

Geometry [mm]	Charge state		
	8+ [μA]	9+ [μA]	11+ [μA]
Diameter = 8	6.7	2.0	0.06
20 × 4	18.0	8.0	0.73
40 × 4	29.0	15.2	1.54

Fig. 3 shows the argon beam currents as a function of the charge state for RF powers of 50–280 W at 10.964 GHz with the 40 mm × 4 mm slit. The measurement parameters were: −2.4 kV puller voltage, 70 V quadrupole Q1 voltage, −12 V biased disc voltage. The measured beam currents demonstrate that the CUBE ion source is RF power limited as the beam currents increase with increasing power without any sign of saturation. Fig. 3 also illustrates that the argon CSD has a local maximum at charge state 8+, which is also visible in Fig. 2. The local maximum is presumably due to the closed electron shell structure of Ar^{8+}, and the significant increase of the ionization potential between charge states 8+ to 9+, causing "pile-up" to 8+. Similar effect, arguably caused by insufficient microwave power, is often observed in charge breeder ion sources where the maximum efficiency corresponds to the charge state with closed electron shell, e.g. K^{9+} being the best comparison to argon (see e.g. Ref. [14]).

3.2. Emittance measurements

The measured (x, x') and (y, y') phase space distributions of Ar^{8+} for each extraction aperture (8 mm diameter round aperture, 20 mm × 4 mm slit and 40 mm × 4 mm slit) are shown in Fig. 4. The corresponding normalized root mean square (rms) emittance values are shown for

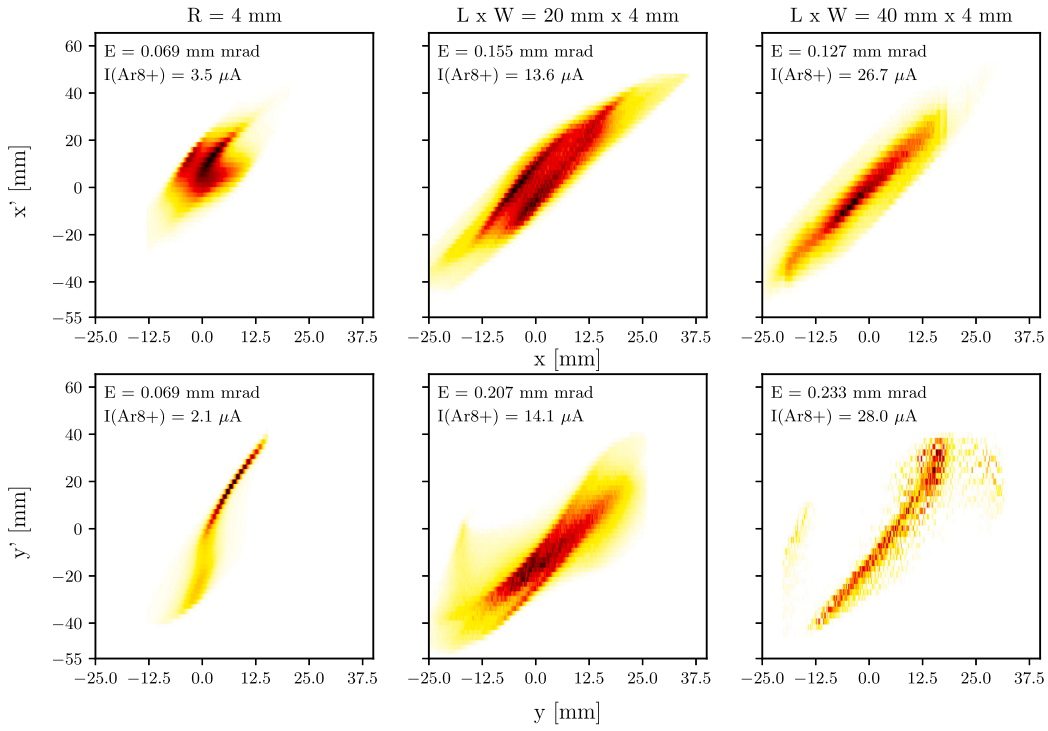

Fig. 4. (x, x') and (y, y') phase space distributions of 80 keV Ar^{8+} beam for each plasma electrode aperture. The high voltage power supply drain currents, which allude to the total extracted beam current, are 0.34 mA for the 8 mm diameter round aperture, approximately 0.38 mA for the 20 mm × 4 mm slit and about 1.4 mA for the 40 mm × 4 mm slit. The corresponding emittance values are normalized rms. The location $x = y = 0$ corresponds to the optical axis of the LEBT.

each case. The phase space distributions indicate that the beam is diverging in both planes at the location of the emittance scanner with all apertures. With the two slit apertures the beam physical and angular dimensions are roughly the same in both planes, which offers a hint that the slit beams, or at least the larger one, are collimated during the beam transport (corroborated by simulations, as will be shown in the subsequent sections). In comparison the round aperture beam is considerably smaller in physical and angular dimensions.

Fig. 5 shows the normalized rms-emittance as a function of the M/Q-ratio of argon for the 40 mm × 4 mm slit extraction in (x, x') and (y, y'). The corresponding RF powers are 234 W and 280 W, respectively. The data were collected applying gas mixing with oxygen and the (negative) puller voltage was 2.6–2.8 kV. In both cases (transverse planes) the beam emittance increases monotonically with increasing charge state (decreasing M/Q), which is in contrast to the behaviour in traditional ECRIS, where for high charge states the emittance decreases with increasing charge state [15–17]. This is arguably caused by the non-uniform distribution of different charge state ions across the extraction aperture, i.e. higher charge states originating near the axis of the (conventional) ECRIS [18].

The normalized rms emittance (y, y') of selected charge states of argon with the 40 mm × 4 mm slit aperture is shown in Fig. 6 as a function of the RF power. The measurement was done with a −2.8 kV puller voltage. The emittance of each charge state is approximately constant for all the RF powers used. For the charge states 4+ and 6+ the emittance varied only by 15% while the beam current almost doubled from 22 μA to 40 μA and from 14 μA to 26 μA, respectively. The emittance of the charge state 8+ varied by 35% as the beam current increased from 10 μA to 28 μA. Finally, the emittance of the charge state 9+ varied by 12% as the beam current more than quadrupled from 3 μA to 13 μA. The total beam current (power source drain current) increased from 1.14 mA to 1.45 mA across the power sweep. The conclusion is that the beam emittance is independent of the (total) beam current, at least with the present LEBT. Nevertheless, the measurements solely capture the emittance of the beam that has been successfully transported through the LEBT, while disregarding the collimated segment of the beam.

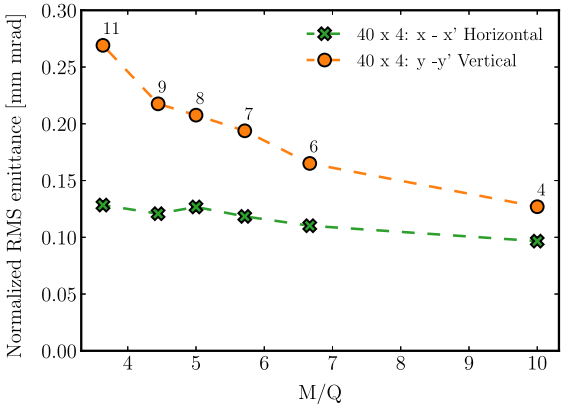

Fig. 5. Normalized rms emittance of argon as a function of the mass-to-charge ratio for the 40 mm × 4 mm rectangular slit aperture (both (x, x') and (y, y')). The argon charge states are 4+, 6+, 7+, 8+, 9+ and 11+. Argon charge state labels accompanying the data points are shown for clarity.

3.3. Beam transport

The transport efficiency of the low energy beamline (from the ion source to the Faraday cup) was studied with helium plasma and −2.6 kV puller voltage using the 40 mm × 4 mm slit extraction aperture. The efficiency was found between 32–50% as a function of the high voltage source drain current (between 0.4 mA and 1.6 mA), which was varied by adjusting the RF power from 4 W to 200 W. The beam intensities with the 200 W RF power are 78 μA and 300 μA for the 2+ and 1+ charge states, respectively. The transport efficiency $\eta = I_{He,f}/I_{He,i}$, where f stands for the final (measured) and i the initial helium beam currents, is calculated by assuming that the efficiency is the same for He and other contamination elements that are present in the extracted beam (mainly oxygen), and then dividing the combined total of the

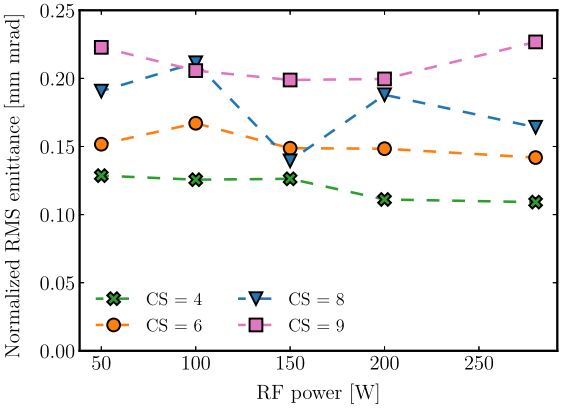

Fig. 6. Normalized rms emittance (y, y') of argon as a function of the RF power for different charge states with 40 mm × 4 mm slit aperture.

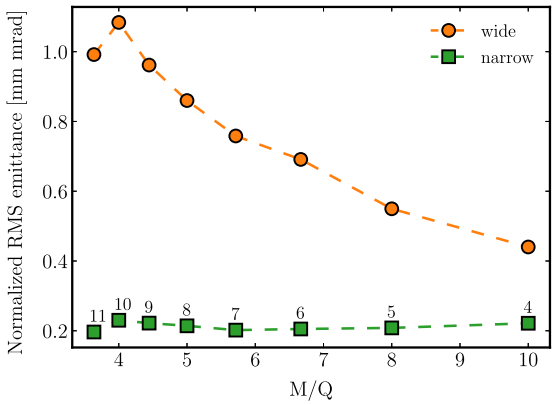

Fig. 7. Simulated normalized rms emittances of argon beams in the CUBE-ECRIS extraction at $z = 300$ mm measured from the ion source B-field minimum. The emittance values are calculated in the directions defined by the beam rotation and are labelled here as *wide* and *narrow* referring to the slit beam dimensions. Argon charge state labels accompanying the data points are shown for clarity.

measured beam currents by the drain current of the ion source high voltage power supply. As the maximum field strength of the dipole magnet is not strong enough to measure the O^+ current at 10 kV, it is approximated by a linear fit using the other measured oxygen charge states. In reality, a certain fraction of the high voltage drain current results from electron backflow, which causes the transport efficiency (calculated as explained above) to be underestimated, i.e. the quoted values represent the minimum transport efficiency.

4. Extraction and beam transport simulations

Two simulation packages were used to model the extraction and beam transport of the CUBE-ECRIS to gain insight into the experimental observations. IBSimu [19] was used to model the ion beam extraction from plasma and PIOL [20] was used for the low energy beam transport simulations.

4.1. Extraction

Beam extraction from the plasma was simulated with IBSimu assuming that the flux of ions at the plasma electrode follows the electron flux produced by the plasma simulations presented in Ref. [1]. This assumption is supported by the observable plasma flux burn mark at the plasma electrode. The flux is almost uniform in the long direction of the slit (horizontal) and has a Gaussian distribution with a standard deviation of 0.5 mm in the vertical direction. The CSD, which is assumed to be independent of the spatial distribution, is defined according to the experimental observations. The other plasma parameters are based on typical values used for ECRIS simulations [21]. The IBSimu simulations take into account space charge effects in the beam region. The beam space charge is compensated in the plasma as defined by the plasma model.

The extracted beam data can be used to evaluate the relative fractions of beam expected to be extracted through different extraction apertures. The extracted currents follow very closely the length of the aperture and are therefore 2.5× for the 20 mm × 4 mm and 5× for the 40 mm × 4 mm slit apertures compared to the round 8 mm diameter aperture. As the magnetic fringe field of the ion source decreases in the extraction region the beam experiences rotation due to the Lorentz force. The slit beam rotates from horizontal to vertical and is collimated within the narrow puller electrode. The beam from 8 mm diameter round aperture has a throughput of 100% with no collimation. For slit apertures, the degree of the collimation depends on the M/Q-ratio, the source voltage and the horizontal length of the beam (long dimension of the slit). The throughput is 97% for the 20 mm × 4 mm aperture and 89% for the 40 mm × 4 mm aperture for Ar^{8+}, extracted with 10 kV potential.

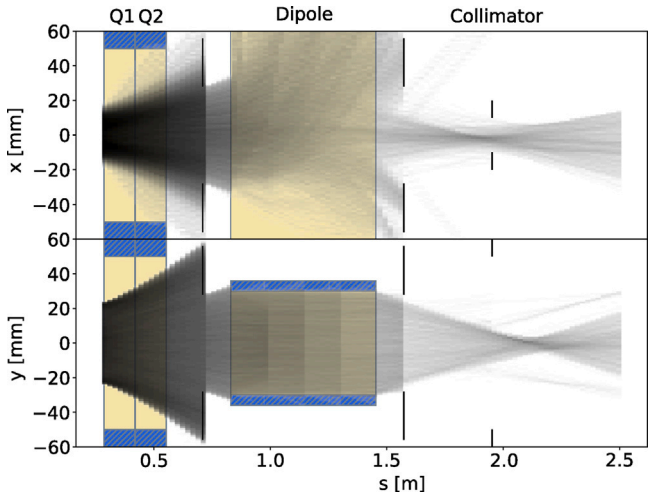

Fig. 8. Profile view of the argon beam extracted from 40 mm × 4 mm slit aperture within the CUBE LEBT, calculated with 0% SCC. The greyscale colours indicate particle density. Dipole is tuned for selecting Ar^{8+} and the other charge states are deflected in x-direction.

Fig. 7 shows the normalized rms emittances in the extraction system at $z = 300$ mm measured from the B-field minimum. The emittances are plotted in the direction defined by the beam rotation, which varies with the M/Q, and are labelled as *wide* and *narrow* referring to the slit beam dimensions. In the narrow dimension, the beam emittance stays approximately constant for all M/Q values. The emittances ranges from 0.2 to 0.22 mm mrad. In the wide direction, the beam emittance values are between 0.45–1.08 mm mrad, i.e. decrease by more than 50% when M/Q increases from 3.6 to 10. This trend is associated with the beam rotation caused by the fringe magnetic field. Such trend has been predicted theoretically for conventional ECR ion sources with round extraction aperture and decreasing solenoid field [22].

4.2. LEBT

The simulation of the following LEBT was made with PIOL [20] using third order matrices and the particle distributions from the extraction simulations. The quadrupole voltages were set to zero to model the experimental conditions. The simulations can include space charge forces from all extracted charge states, which can be especially significant before the separation in the dipole. As the degree

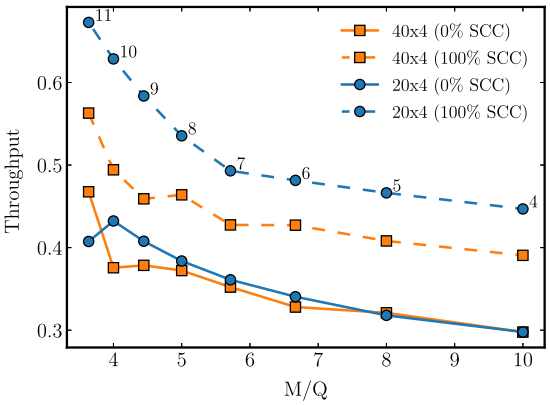

Fig. 9. Throughput of simulated argon beams (charge states) from the plasma electrode to the FC with 0 and 100% space charge compensation degree. Argon charge state labels accompanying the data points are shown for clarity.

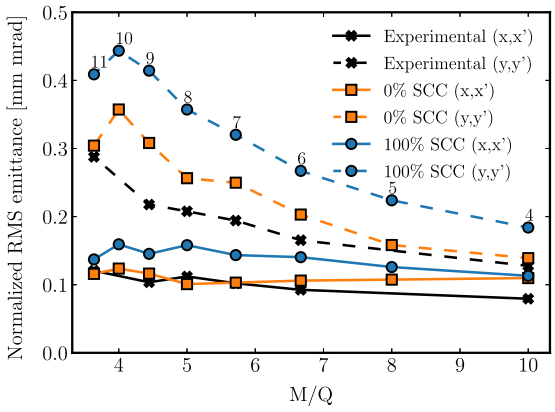

Fig. 10. Simulated (y, y') and (x, x') emittances of argon beams as a function of the mass-to-charge ratio at the location of the emittance scanner with (0% SCC) and without beam space charge (100% SCC). Measured beam emittances from Fig. 5 are shown for reference and argon charge state labels accompanying the data points are shown for clarity.

of space charge compensation (SCC) in the LEBT is not known, the LEBT simulations were done with both, 100% SCC (no space charge effects), and 0% SCC (full space charge forces). The true experimental condition is somewhere in between these extremes. Fig. 8 shows the projection of the argon beam (all charge states) extracted from the 40 mm × 4 mm slit aperture and calculated with 0% SCC. Here the dipole is set to transport Ar^{8+} ions. Significant beam collimation occurs downstream from the quadrupole chamber. The throughput from the plasma electrode to the FC is presented in Fig. 9 for both slit extraction apertures used in the experiments, and SCC-factors of 0 and 100%. According to the simulations it can be expected that e.g. the Ar^{8+} transport efficiency is between 33 and 41% for the 40 mm × 4 mm slit aperture. Throughput of the 20 mm × 4 m slit aperture follows the same trend as the bigger slit, but with systematically higher throughput in the 100% SCC case.

The effect of the collimation can also be seen in the transverse rms emittance values evaluated for the argon charge states at the location of the experimental emittance scans at $s = 2.5$ m presented in Fig. 10 for both 0 and 100% SCC cases. The intermediate SCC degrees lead to emittance values between these two extremes. The 0% SCC yields smaller emittances because the beam is collimated more. The measured emittance values from Fig. 5 are shown for reference. It can be seen that the simulated emittance is larger than the observed emittance. Therefore, it can be concluded that the simulation does not fully correspond to the experiment. The reasons for this could be related to the plasma model used for the extraction but remain elusive.

The LEBT simulations were also used to predict the transport efficiency for helium beams with total intensities of 0.5, 1.0 and 1.5 mA in the 40 mm × 4 mm slit aperture case. The simulated efficiencies are presented together with the experimental data (see Section 3.3) in Fig. 11. The transport efficiencies for the 100% SCC case are between 45–50% and 9–21% for the 0% SCC case. The large contrast between these extremes is due to the considerable collimation with the 0% SCC case as discussed previously. The measured transport efficiency is considerably better than the 0% SCC case and almost as high as the 100% SCC case. Finally, we note that in the experiment the SCC degree could be affected by the electrostatic quadrupoles. However, if the quadrupole voltages are optimized in the LEBT simulations, they indicate that the beam transmission increases significantly. For example, the Ar^{8+} transmission increases from the values presented in Fig. 9 (33% and 42% for SCC 0% and 100% respectively) up to 74% in both cases. The transport efficiency is insensitive to the SCC-factor at optimized quadrupole voltages. Only a slight tuning of the focusing power is sufficient to compensate for the space charge forces. Nevertheless, such behaviour was not observed experimentally.

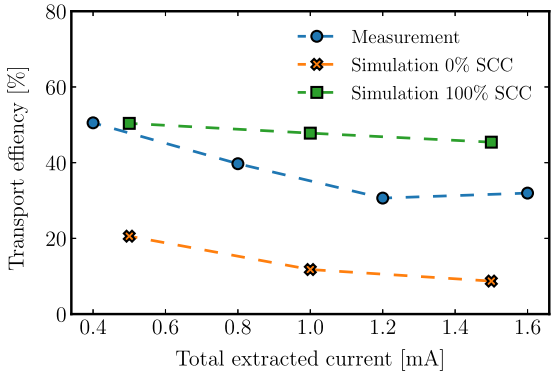

Fig. 11. Measured and simulated (combined IBSimu and PIOL with 0 and 100% SCC) transport efficiency of helium beam (charge states 1+ and 2+ combined) as a function of the high voltage power supply drain current (measurement) or total extracted current (simulation).

5. Discussion

The experimental results shown in this study demonstrate that the ion beams produced with the minimum-B quadrupole ECRIS using a rectangular slit extraction aperture can be successfully transported through the LEBT. Furthermore, the beam intensities produced with the rectangular slit apertures increase considerably compared to the round extraction aperture, which is to be expected based on the earlier plasma flux simulation reported in Ref. [1].

The argon beam current intensities of the CUBE-ECRIS can be compared to those achieved with (a) conventional (electromagnet solenoid + permanent magnet sextupole) ECR ion sources operating at ~10 GHz frequency, (b) all permanent-magnet ECR ion sources operating at ~10 GHz frequency, and (c) other ECR ion sources with unconventional magnetic field topologies. For (a) the benchmark device is the 10 GHz coaxially coupled Caprice ion source producing 36 μA of Ar^{9+} when operating with a single microwave frequency [23] (unknown RF power or source potential complicating the comparison). The record Ar^{9+} beam current of 15 μA achieved with the CUBE-ECRIS is smaller by a factor of almost 3. However, we expect to bridge this gap in performance with further improvements of the CUBE-ECRIS outlined below. In category (b) we compare the CUBE-ECRIS to 10 GHz and 14.5 GHz NANOGAN devices producing 5 μA and 20 μA of Ar^{9+}, respectively [24]. Here the CUBE-ECRIS compares well with the commercial all permanent-magnet ECR ion sources. Finally, in category (c) the CUBE-ECRIS has

already delivered higher argon charge states, i.e. up to Ar^{11+}, than other ECR ion sources with unconventional magnetic field topologies, i.e. the 6.4 GHz ARC-ECRIS [6] with (electromagnet) minimum-B quadrupole structure and the 10 GHz PM ring ECRIS, PK-GANESA [25], producing charge states up to Ar^{6+} and Ar^{3+}, respectively. The argon charge state distributions of the CUBE-ECRIS and the Quadrumafios source [7] are rather similar. Both sources have achieved >1 μA Ar^{11+} beams. CUBE-ECRIS accomplished this with ~300 W, and Quadrumafios with 2 kW of microwave power at 10 GHz. However, direct comparison of the performance is challenging due to the different extraction systems (Quadrumafios uses a round extraction aperture) and the different microwave powers. The apparent performance difference to conventional minimum-B ECR ion sources with solenoid and sextupole fields is enticing the conclusion that high charge state production in plasma of the quadrupole minimum-B configuration is inferior. However, such conclusion would be premature since the plasma transport into the extraction aperture has not been optimized in the quadrupole devices, e.g. by optimizing the location and shape of the extraction aperture with respect to the magnetic field whereas traditional ECR ion sources benefit from long history of development culminating to dedicated experiments on this matter (see Ref. [26], for example).

The emittance measurements reveal a particular trend, where the emittance increases monotonically with increasing charge state (decreasing M/Q) in both measurement planes. This is associated to the diverging magnetic field in the extraction, which also causes the beam to rotate (see Section 4.1). In contrast, conventional ECR ion sources exhibit the opposite behaviour i.e. for high charge states the emittance decreases with increasing charge state, which is typically attributed to non-uniform charge-state distribution across the extraction aperture, as discussed in Section 3.2, i.e. the high charge state ions occupying the volume near the source axis. In the case of CUBE-ECRIS, the high charge states are extracted uniformly across the entire width of the aperture, rather than just from the centre. Therefore, there are no distinct "effective aperture radii" for different charge state ions in CUBE-ECRIS, or at least we have not observed any evidence of such effect. The data presented in Table 1 cannot be used to make such conclusions due to different plasma conditions used in the experiments. The transport efficiencies, discussed in Section 4.2, also exhibit a dependence on the mass-to-charge ratio, which could influence the emittance results. The transport efficiency increases as a function of decreasing M/Q-ratio, meaning that higher charge states have better throughput. Lower transport efficiency indicates more severe collimation in the LEBT, which can presumably result in smaller emittance compared to less collimation/higher charge state. Hence, both factors i.e. the beam rotation and transport efficiency can affect the measured emittance trends, and their contributions cannot be separated

Lastly, the obtained emittance values are comparable to those of conventional ECR ion sources. For example, the typical normalized rms emittance values measured with the JYFL 14 GHz ECR ion source for Ar^{8+} beams produced with N_2 mixing gas and 10 kV extraction, are 0.07–0.14 mm mrad depending on the ion source and beamline settings [27]. These values have been measured with the same emittance scanner that was used in the studies presented here. This similarity in emittance values between the conventional ECRIS (round 8 mm aperture) and CUBE-ECRIS with a slit aperture further supports the viability of the unconventional magnetic field topology for future development, such as the proposed superconducting ARC-ECRIS [8].

This study highlights two avenues for improving the beam intensities of the CUBE-ECRIS: increased RF power and better LEBT beam transport. Fig. 3 shows that the beam intensities increase monotonically with added RF power, which suggests that more than 300 W is required for optimizing the high charge state beam production similar to conventional ECR ion sources. The transport efficiency is mainly limited by the mismatch of the beams into the acceptance of the dipole magnet. This is understood to be caused by the electrostatic quadrupole doublet not providing the expected focusing effect for reasons that remain elusive. We target to address the transport issue by implementing one or more of the following changes in the LEBT in the future; replacing the electrostatic quadrupole doublet with an electromagnet version, increasing the dipole magnet pole gap (acceptance), and/or shortening the drift between the ion source and the dipole magnet thus eliminating the need for quadrupole focusing to control the beam size.

CRediT authorship contribution statement

Sami Kosonen: Conceptualization, Investigation, Methodology, Formal analysis, Software, Writing – original draft, Visualization, Writing – review & editing. **Taneli Kalvas:** Funding acquisition, Conceptualization, Investigation, Resources, Formal analysis, Software, Writing – original draft, Visualization, Writing – review & editing. **Hannu Koivisto:** Funding acquisition, Project administration, Conceptualization, Investigation, Writing – review & editing. **Olli Tarvainen:** Funding acquisition, Conceptualization, Investigation, Writing – original draft, Writing – review & editing. **Ville Toivanen:** Conceptualization, Investigation, Writing – original draft, Visualization, Writing – review & editing, Data curation.

Declaration of competing interest

The authors declare that they have no known competing financial interests or personal relationships that could have appeared to influence the work reported in this paper.

Data availability

Data available at https://doi.org/10.23729/c5abab71-5277-48d6-a9c2-78101bf58e70.

Acknowledgements

This work has been supported by the Academy of Finland Project funding (N:o 315855).

References

[1] T. Kalvas, O. Tarvainen, V. Toivanen, H. Koivisto, Design of a 10 GHz minimum-B quadrupole permanent magnet electron cyclotron resonance ion source, J. Instrum. 15 (2020) P06016.
[2] T. Kalvas, V. Toivanen, S.T. Kosonen, H. Koivisto, O. Tarvainen, L. Maunoury, First results of a new quadrupole minimum-B permanent magnet electron cyclotron resonance ion source, Plasma Sources. Sci. Technol. 31 (2022) 12LT02.
[3] G. Porter, M. Rensink, Plasma modeling of MFTF-B and the sensitivity to vacuum conditions, J. Vac. Sci. Technol. A 3 (1985) 1157–1160.
[4] M. Inutake, et al., Thermal barrier formation and plasma confinement in the axisymmetrized tandem mirror GAMMA 10, Phys. Rev. Lett. 55 (1985) 939.
[5] C. Petty, D. Smith, D. Smatlak, Time-of-flight analyzer for ion end loss of a mirror plasma, Rev. Sci. Instrum. 59 (1988) 601–604.
[6] P. Suominen, T. Ropponen, H. Koivisto, First results with the yin-yang type electron cyclotron resonance ion source, Nucl. Instrum. Methods A 578 (2007) 370–378.
[7] A. Girard, P. Briand, G. Gaudart, J. Klein, F. Bourg, J. Debernardi, J. Mathonnet, G. Melin, Y. Su, The quadrumafios electron cyclotron resonance ion source: Presentation and analysis of the results, Rev. Sci. Instrum. 65 (1994) 1714.
[8] P. Suominen, F. Wenander, Electron cyclotron resonance ion sources with arc-shaped coils, Rev. Sci. Instrum. 79 (2008) 02A305.
[9] O. Tarvainen, T. Kalvas, V. Toivanen, S. Kosonen, H. Koivisto, C. Hill, A. Bainbridge, A. Hinton, B. Shepherd, D. Faircloth, Ion source and low energy beam transport prototyping for a single-ended heavy ion ToF-ERDA facility, Nucl. Instrum. Methods Phys. Res. B. 538 (2023) 110–114.
[10] O. Allison, J. Sherman, D. Holtkamp, An emittance scanner for intense low-energy ion beams, IEEE Trans. Nucl. Sci. 30 (1983) 2204–2206.
[11] T. Kalvas, Ion beam intensity and phase space measurement techniques for ion sources, Rev. Sci. Instrum. 93 (2022) 011501.
[12] M. Stockli, R. Whelton, R. Keller, A. Letchford, R. Thomae, J. Thomason, Accurate estimation of the RMS emittance from single current amplifier data, in: AIP Conf. Proc. Vol. 639, 2002, pp. 135–159.
[13] G. Hahn, T. Yang, H. You, J. Hwang, Design and experimental validation of high-resolution single-shot emittance diagnostics for heavy-ion beams, IEEE Trans. Instrum. Meas. 70 (2021) 1–7.

[14] M. Luntinen, V. Toivanen, H. Koivisto, J. Angot, T. Thuillier, O. Tarvainen, G. Gastro, Diagnostics of highly charged plasmas with multicomponent 1+ ion injection, Phys. Rev. 106 (2022) 055208.
[15] M. Leitner, D. Wutte, C. Lyneis, Diagnostics of highly charged plasmas with multicomponent 1+ ion injection, in: Proceedings of the 2001 Particle Accelerator Conference, 2001.
[16] D. Leitner, D. Winklehner, M. Strohmeier, Ion beam properties for ECR ion source injector systems, J. Instrum. 6 (2011) P07010.
[17] J. Mandin, Étude expérimentale et simulation des conditions d'extraction d'un faisceau d'ions multi-chargés d'une source à résonance cyclotronique électronique (Ph.D. thesis), Caen University thesis, 1996.
[18] L. Panitzsch, T. Peleikis, S. Böttcher, M. Stalder, Current density distributions and sputter marks in electron cyclotron resonance ion sources, Rev. Sci. Instrum. 84 (2013) 013303.
[19] T. Kalvas, O. Tarvainen, T. Ropponen, O. Steczkiewicz, J. Ärje, H. Clark, IBSIMU: A three-dimensional simulation software for charged particle optics, Rev. Sci. Instrum. 81 (2010) 02B703.
[20] T. Kalvas, J. Sarén, W. Gins, PIOL - Python-driven Ion Optics Library, University of Jyväskylä, Department of Physics, 2020.
[21] V. Toivanen, T. Kalvas, H. Koivisto, J. Komppula, O. Tarvainen, Double einzel lens extraction for the JYFL 14 GHz ECR ion source designed with IBSimu, J. Instrum. 8 (2013) P05003.
[22] G. Brewer, in: A. Septier (Ed.), Focusing of High-Density Electron Beams, in Focusing of Charged Particles. Vol. II, Academic Press, New York U.S.A., 1967, pp. 76–121.
[23] B. Jacquot, M. Pontonnier, La source CAPRICE 10 GHz en mode harmonique $2(\omega_{HF} - \omega_{CE} = 0)$, Nucl. Instrum. Methods A 287 (1990) 341–347.
[24] Pantechnik website, http://www.pantechnik.com/.
[25] P. Salou, L. Maunoury, G. Gaubert, M. Michel, N. Lecesne, R. Leroy, D. Besnier, PK-GANESA: An ECRIS for testing the axisymetric magnetic structure for the production of multicharged ion beams, in: AIP Conf. Proc. Vol. 2011, 2018, p. 040021.
[26] Y. Higurashi, T. Nakagawa, M. Kidera, T. Aihara, K. Kobayashi, M. Kase, A. Goto, Y. Yano, Effect of the plasma electrode position and shape on the beam intensity of the highly charged ions from RIKEN 18 GHz electron-cyclotron-resonance ion source, Japan. J. Appl. Phys. 44 (2005) 5216.
[27] V. Toivanen, O. Steczkiewicz, O. Tarvainen, J. Ropponen, J. Ärje, H. Koivisto, The effects of beam line pressure on the beam quality of an electron cyclotron resonance ion source, Nucl. Instrum. Meth. B 268 (2010) 1508–1516.